Global Fits of Dirac Dark Matter Effective Field Theories

Ankit Beniwal

(On behalf of the GAMBIT Collaboration)

P. Athron et al., *Thermal WIMPs and the Scale of New Physics: Global Fits of Dirac Dark Matter Effective Field Theories*, *EPJC* 81 (2021) 11, 992, [arXiv:2106.02056]

Outline

1. Global fits and GAMBIT
2. Dirac fermion DM EFTs
3. Constraints and likelihoods
4. Results
5. Summary

Global fits and GAMBIT

Theories with *many* free parameters/constraints?

1. Construct a *composite likelihood* function:

$$\mathcal{L}_{\text{total}} = \mathcal{L}_{\text{DD}} \times \mathcal{L}_{\text{ID}} \times \mathcal{L}_{\text{Collider}} \times \ldots$$

2. Traditional sampling methods (random, grid) are inefficient. S. S. AbdusSalam et al., [arXiv:2012.09874]
3. Explore parameter space using *advanced* sampling techniques (e.g., MCMC, nested sampling).
4. Interpret results in *frequentist* and/or *Bayesian* statistical frameworks.

→ **GAMBIT**

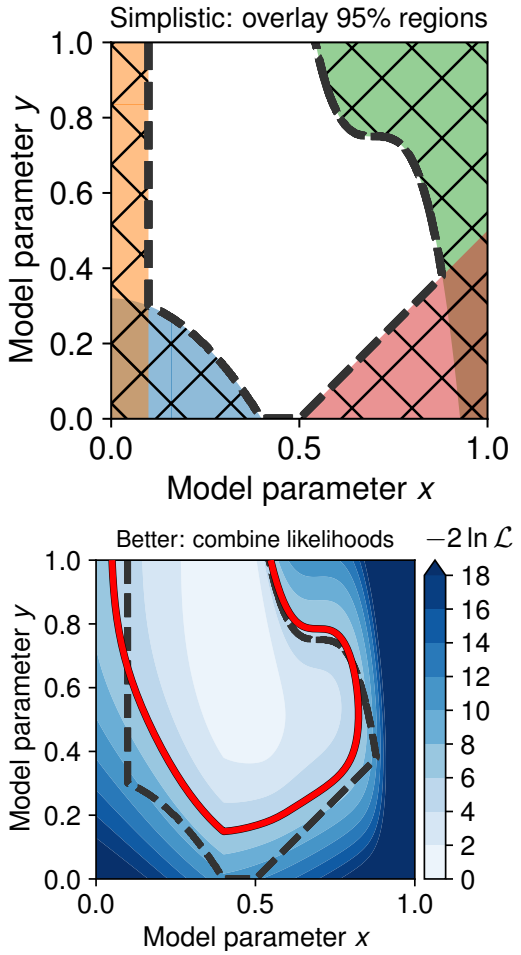

GAMBIT: The Global And Modular BSM Inference Tool

gambit.hepforge.org github.com/GambitBSM EPJC 77 (2017) 784 arXiv:1705.07908

- Extensive model database, beyond SUSY
- Fast definition of new datasets, theories
- Extensive observable/data libraries
- Plug&play scanning/physics/likelihood packages
- Various statistical options (frequentist /Bayesian)
- Fast LHC likelihood calculator
- Massively parallel
- Fully open-source

Members of: ATLAS, Belle-II, CLiC, CMS, CTA, Fermi-LAT, DARWIN, IceCube, LHCb, SHiP, XENON

Authors of: BubbleProfiler, Capt'n General, Contur, DarkAges, DarkSUSY, DDCalc, DirectDM, Diver, EasyScanHEP, ExoCLASS, FlexibleSUSY, gamLike, GM2Calc, HEPLike, IsaTools, MARTY, nuLike, PhaseTracer, PolyChord, Rivet, SOFTSUSY, SuperIso, SUSY-AI, xsec, Vevacious, WIMPSim

Recent collaborators: P Athron, C Balázs, A Beniwal, S Bloor, T Bringmann, A Buckley, J-E Camargo-Molina, C Chang, M Chrzaszcz, J Conrad, J Cornell, M Danninger, J Edsjö, T Emken, A Fowlie, T Gonzalo, W Handley, J Harz, S Hoof, F Kahlhoefer, A Kvellestad, P Jackson, D Jacob, C Lin, N Mahmoudi, G Martinez, MT Prim, A Raklev, C Rogan, R Ruiz, P Scott, N Serra, P Stöcker , W. Su, A Vincent, C Weniger, M White, Y Zhang, ++

70+ participants in many experiments and numerous major theory codes

Recent GAMBIT studies

Higgs-portal DM

[Eur.Phys.J.C 79 (2019) 1, 38]

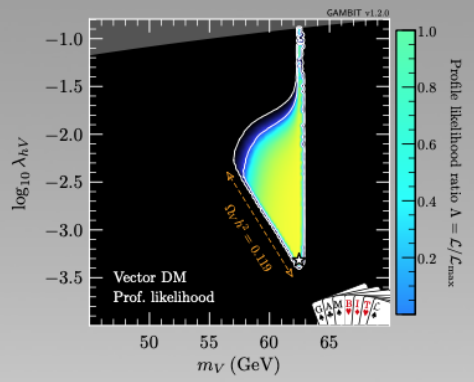

MSSM-EW

[Eur.Phys.J.C 79 (2019) 5, 395]

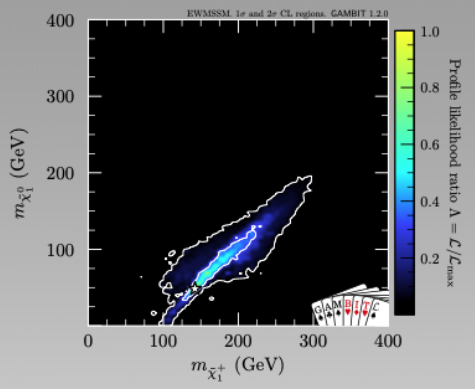

Right-Handed Neutrinos

[Eur.Phys.J.C 80 (2020) 6, 569]

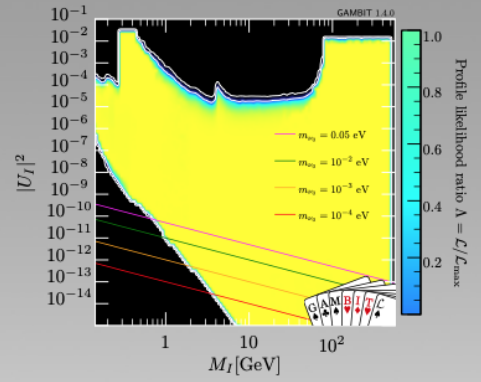

Flavour EFT

[arXiv:2006.03489 hep-ph]

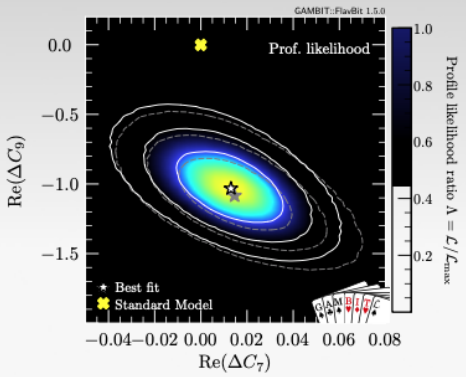

DM ALPs

[arXiv:2007.05517 astro-ph.CO]

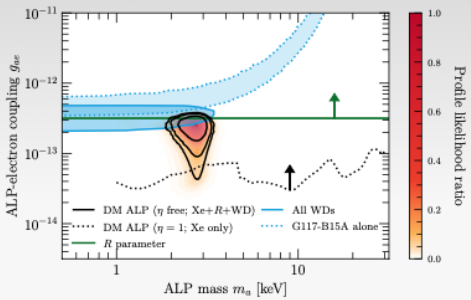

Neutrino Masses

[arXiv:2009.03287 astro-ph.CO]

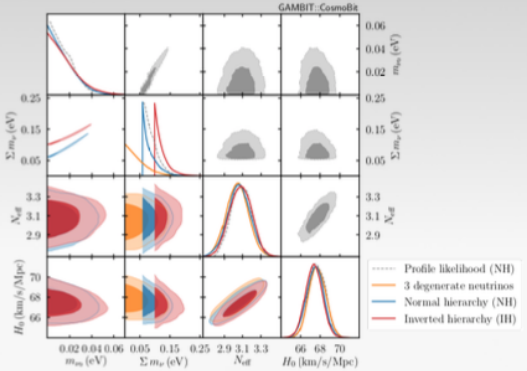

Slide from T. Gonzalo, Moriond 2021

- A Dirac fermion WIMP DM (χ) interacting with SM quarks or gluons via

$$\mathcal{L}_{\text{int}} = \sum_{a,d} \frac{\mathcal{C}_a^{(d)}}{\Lambda^{d-4}} \mathcal{Q}_a^{(d)} \,, \tag{1}$$

where $\mathcal{C}_a^{(d)}$ = dimensionless Wilson coefficients, Λ = scale of new physics, $d \leq 7$ and $\mathcal{Q}_a^{(d)}$ = DM-SM operators.

- Full Lagrangian is

$$\mathcal{L} = \mathcal{L}_{\text{SM}} + \mathcal{L}_{\text{int}} + \overline{\chi}(i\partial\!\!\!/ - m_\chi)\chi \,. \tag{2}$$

- Free model parameters:

$$6 \ (d=6), \quad 16 \ (d=6 \ \& \ 7) \,.$$

Dimension-6 operators

$$\begin{aligned}
\mathcal{Q}_{1,q}^{(6)} &= (\overline{\chi}\gamma_\mu\chi)(\overline{q}\gamma^\mu q) \,, \\
\mathcal{Q}_{2,q}^{(6)} &= (\overline{\chi}\gamma_\mu\gamma_5\chi)(\overline{q}\gamma^\mu q) \,, \\
\mathcal{Q}_{3,q}^{(6)} &= (\overline{\chi}\gamma_\mu\chi)(\overline{q}\gamma^\mu\gamma_5 q) \,, \\
\mathcal{Q}_{4,q}^{(6)} &= (\overline{\chi}\gamma_\mu\gamma_5\chi)(\overline{q}\gamma^\mu\gamma_5 q) \,.
\end{aligned}$$

Dimension-7 operators

$$\begin{aligned}
\mathcal{Q}_1^{(7)} &= \frac{\alpha_s}{12\pi}(\overline{\chi}\chi)G^{a\mu\nu}G^a_{\mu\nu} \,, \\
\mathcal{Q}_2^{(7)} &= \frac{\alpha_s}{12\pi}(\overline{\chi}i\gamma_5\chi)G^{a\mu\nu}G^a_{\mu\nu} \,, \\
\mathcal{Q}_3^{(7)} &= \frac{\alpha_s}{8\pi}(\overline{\chi}\chi)G^{a\mu\nu}\widetilde{G}^a_{\mu\nu} \,, \\
\mathcal{Q}_4^{(7)} &= \frac{\alpha_s}{8\pi}(\overline{\chi}i\gamma_5\chi)G^{a\mu\nu}\widetilde{G}^a_{\mu\nu} \,, \\
\mathcal{Q}_{5,q}^{(7)} &= m_q(\overline{\chi}\chi)(\overline{q}q) \,, \\
\mathcal{Q}_{6,q}^{(7)} &= m_q(\overline{\chi}i\gamma_5\chi)(\overline{q}q) \,, \\
\mathcal{Q}_{7,q}^{(7)} &= m_q(\overline{\chi}\chi)(\overline{q}i\gamma_5 q) \,, \\
\mathcal{Q}_{8,q}^{(7)} &= m_q(\overline{\chi}i\gamma_5\chi)(\overline{q}i\gamma_5 q) \,, \\
\mathcal{Q}_{9,q}^{(7)} &= m_q(\overline{\chi}\sigma^{\mu\nu}\chi)(\overline{q}\sigma_{\mu\nu}q) \,, \\
\mathcal{Q}_{10,q}^{(7)} &= m_q(\overline{\chi}i\sigma^{\mu\nu}\gamma_5\chi)(\overline{q}\sigma_{\mu\nu}q) \,.
\end{aligned}$$

Constraints and likelihoods

- **Mixing and threshold corrections:**
  - For direct detection, $\mathcal{C}_a^{(d)}$'s required at energy scale $\mu = 2\,\text{GeV}$;
  - Running/mixing of operators handled by DirectDM v2.2.0.

    F. Bishara et al., [arXiv:1708.02678]; J. Brod et al., *JHEP*, [arXiv:1710.10218]
  - Threshold corrections when μ is below/above a quark mass, e.g., m_t.
- **EFT validity:**
  1. $\Lambda \gtrsim 2\,\text{GeV}$ (direct detection);
  2. $\Lambda > 2m_\chi$ (relic density and indirect detection);
  3. $\not{E}_T < \Lambda$ (collider searches). Modify $\not{E}_T$ spectrum when $\not{E}_T > \Lambda$:

$$\frac{d\sigma}{d\not{E}_T} \to \begin{cases} 0\,, & \text{hard cut-off}\,, \\ \dfrac{d\sigma}{d\not{E}_T}\left(\dfrac{\not{E}_T}{\Lambda}\right)^{-a}\,, & \text{smooth cut-off}\,. \end{cases} \tag{3}$$

  Here $a \in [0,\, 4]$ = nuisance parameter.
- **Perturbative couplings:** $|\mathcal{C}_a^{(d)}| < 4\pi$.
- **Parameter ranges:** $m_\chi \in [5,\, 500]\,\text{GeV}$ and $\Lambda \in [20,\, 2000]\,\text{GeV}$.

Constraints and likelihoods

1. **Direct detection** (DirectDM v2.2.0 & DDCalc v2.2.0)

   XENON1T; LUX (2016); PandaX (2016) and (2017); CDMSlite; CRESST-II and CRESST-III; PICO-60 (2017) and (2019); DarkSide-50

   F. Bishara et al., [arXiv:1708.02678]; J. Brod et al., *JHEP*, [arXiv:1710.10218]; P. Athron et al., *EPJC*, [arXiv:1808.10465]

2. **Relic density** (CalcHEP v3.6.27, GUM & DarkSUSY v6.2.2)

   A. Belyaev et al., *CPC.*, [arXiv:1207.6082]; S. Bloor et al., [arXiv:2107.00030]; T. Bringmann et al., *JCAP*, [arXiv:1802.03399]

3. ***Fermi*-LAT via gamma rays** (gamLike v1.0.1) T. Bringmann et al., *EPJC*, [arXiv:1705.07920]

4. **Solar capture** (Capt'n General) and **CMB bounds** (CosmoBit)

   N. Avis Kozar et al., arXiv:[2105.06810]; J. J. Renk et al., *JCAP*, [arXiv:2009.03286]

5. **ATLAS** and **CMS monojet searches** (ColliderBit, FeynRules v2.0, MadGraph_aMC@NLO v2.6.6, Pythia v8.1 & Delphes v3.4.2)

   G. Aad et al., [arXiv:2102.10874]; A. M. Sirunyan et al., *PRD*, [arXiv:1712.02345]
   C. Balazs et al., *EPJC*, [arXiv:1705.07919]; A. Alloul et al., *CPC*, [arXiv:1310.1921]
   J. Alwall et al., *JHEP*, [arXiv:1106.0522]; T. Sjostrand et al., *CPC*, [arXiv:0710.3820]
   J. de Favereau et al., *JHEP*, [arXiv:1307.6346]

\+ **8 nuisance parameters**

Top-quark running mass, nuclear form factors, and astrophysical distribution of DM.

Results

Capped $\mathcal{L}_{\rm LHC}$ likelihood (hard cut-off), $f_\chi \equiv (\Omega_\chi + \Omega_{\overline{\chi}})/0.12 \leq 1$

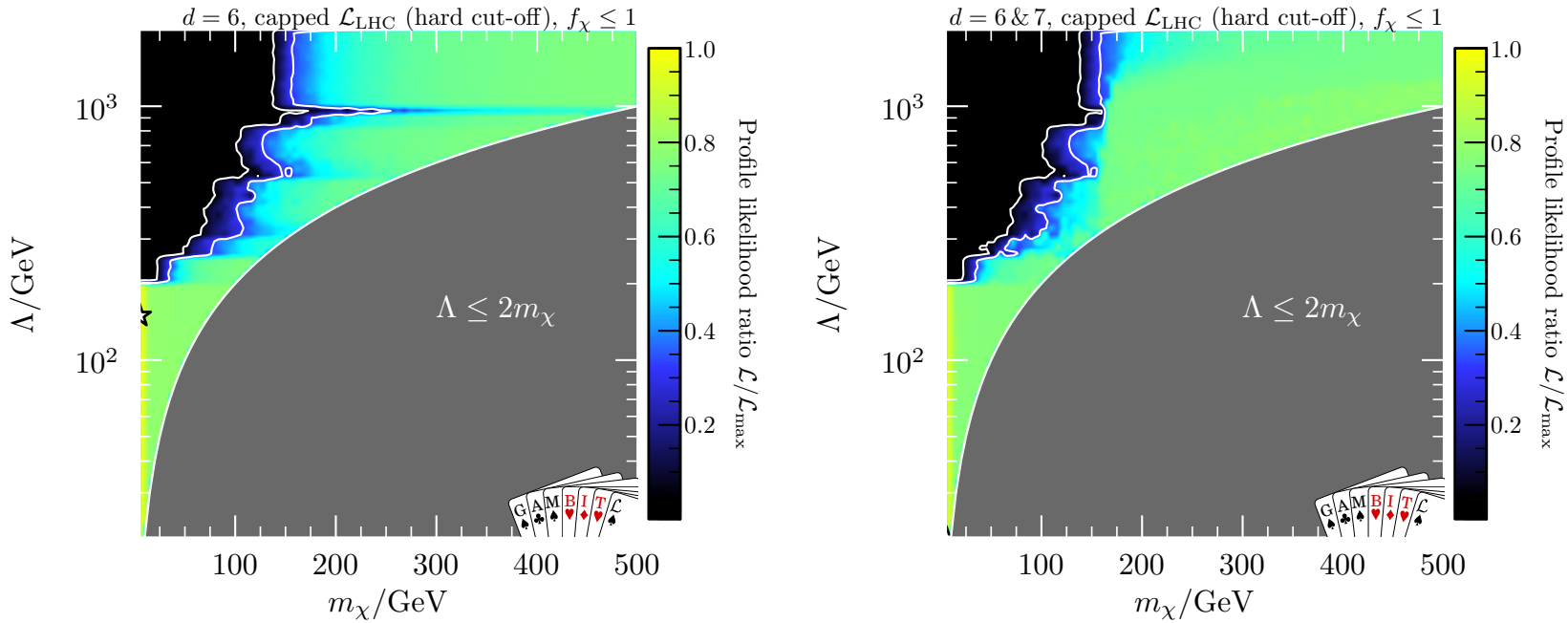

Left panel: $d = 6$; **Right panel**: $d = 6$ & 7; **White star** = best-fit point.

- Small m_χ and large Λ: strong constraints from LHC; impossible to satisfy relic density requirement. LHC constraints absent for $\Lambda < 200\,\text{GeV}$.
- Slight upward fluctuation in *Fermi*-LAT data fitted by (for $d = 6$ case):

$$m_\chi = 5.0\,\text{GeV}, \quad f_\chi^2 \langle \sigma v \rangle_0 = 1.1 \times 10^{-27}\,\text{cm}^3\,\text{s}^{-1}\,. \tag{4}$$

Capped $\mathcal{L}_{\rm LHC}$ likelihood (hard cut-off), $f_\chi \approx 1$

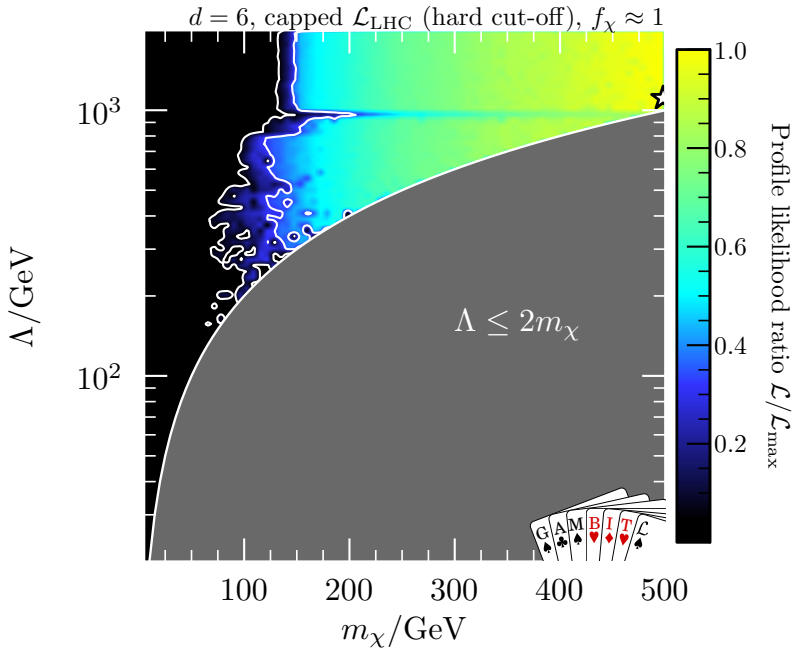

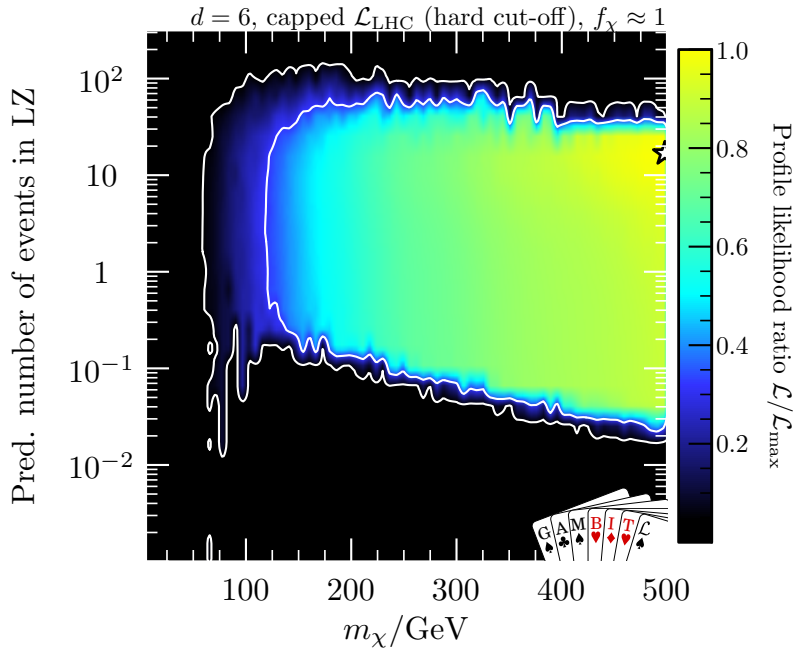

- Impossible to obtain $\Omega_\chi h^2 = 0.12$ for $m_\chi \lesssim 100\,\text{GeV}$; relic density requirement incompatible with *Fermi*-LAT and CMB bounds.
- Up to **10 events** predicted in LZ experiment $\sim$ best-fit point $\rightarrow$ require a non-zero $\mathcal{Q}_2^{(6)}$ (spin-independent, momentum-suppressed interaction).

Full $\mathcal{L}_{\rm LHC}$ likelihood (hard cut-off), $f_\chi \leq 1$

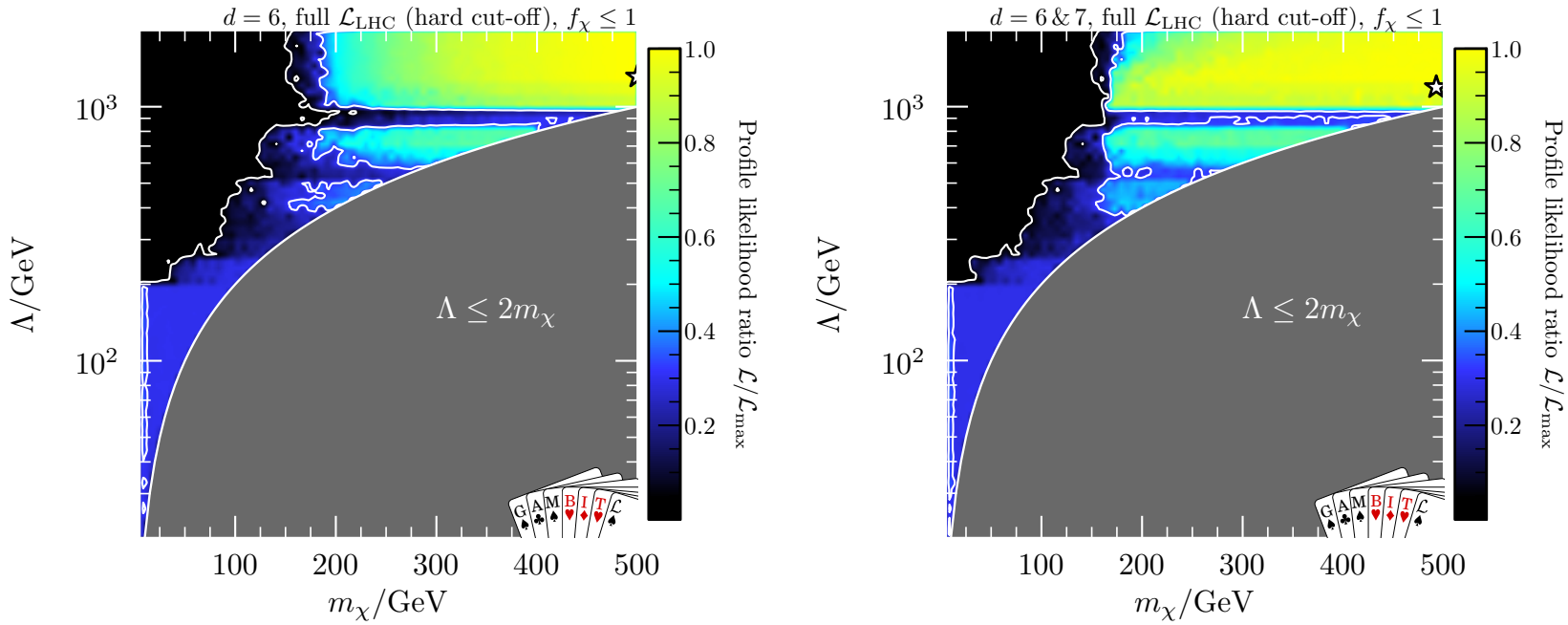

- For $d = 6$, excesses seen in few high-$\not{E}_T$ bins in the ATLAS & CMS monojet searches. Preferred values for Λ at 1σ level:

$$\Lambda \approx 700\ \text{GeV (CMS)}, \quad \Lambda \gtrsim 1\ \text{TeV (ATLAS)}\,. \tag{5}$$

- Similar results for $d = 6$ & 7 (right panel).

Full $\mathcal{L}_{\rm LHC}$ likelihood (smooth cut-off), $f_\chi \leq 1$

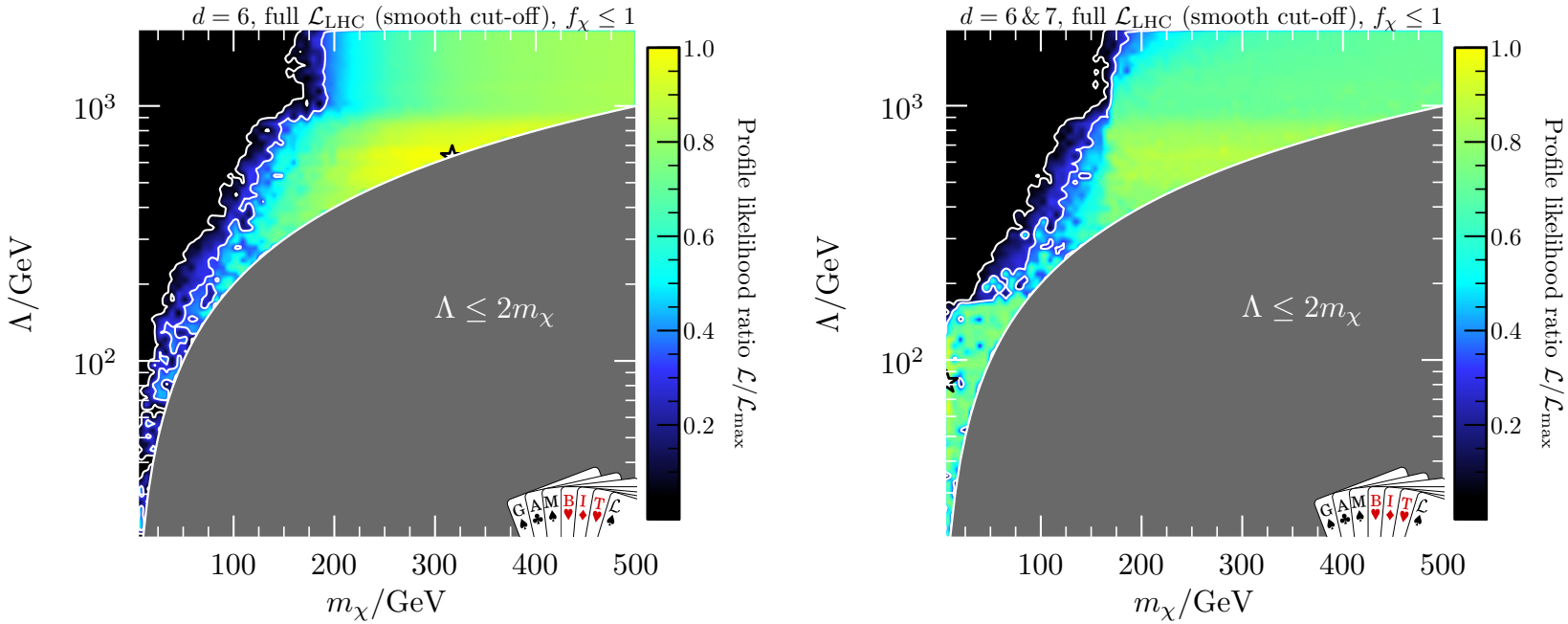

- For $d = 6$, best-fit improves fit to both excesses (*Fermi*-LAT and LHC) simultaneously than in hard cut-off case (similar for $d = 6$ & 7).
- Requires $\Lambda \sim 80\,\text{GeV}$ and soft cut-off $a \approx 1.7$ in the $\not{E}_T$ spectrum.

Summary

- *First* global analysis of full set of effective operators ($d \leq 7$) for a Dirac fermion DM interaction with quarks/gluons.
- Novel approach addresses issue of EFT validity @ LHC via a cut-off parameter for $\not{E}_T > \Lambda$.
- Highly efficient likelihood calculations + sampling algorithms to sample 24 dimensions (m_χ, Λ, 14 x $\mathcal{C}_a^{(d)}$ + 8 nuisance parameters).
- Strong constraints on small m_χ and large $\Lambda \rightarrow$ slight preference for DM signal at relatively small Λ.
- **Large hierarchy *not* possible between m_χ and Λ without violating the relic density constraint.**
- LHC constraints require $\Lambda \lesssim 200\,\text{GeV}$ for $m_\chi \lesssim 100\,\text{GeV}$.
- **Large viable regions of parameter space for $f_\chi \lesssim 1$.**

All results, samples + input files publicly available via Zenodo:

https://zenodo.org/record/4836397

Backup slides

Supplementary results

Capped $\mathcal{L}_{\rm LHC}$ likelihood (hard cut-off), $f_\chi \leq 1$

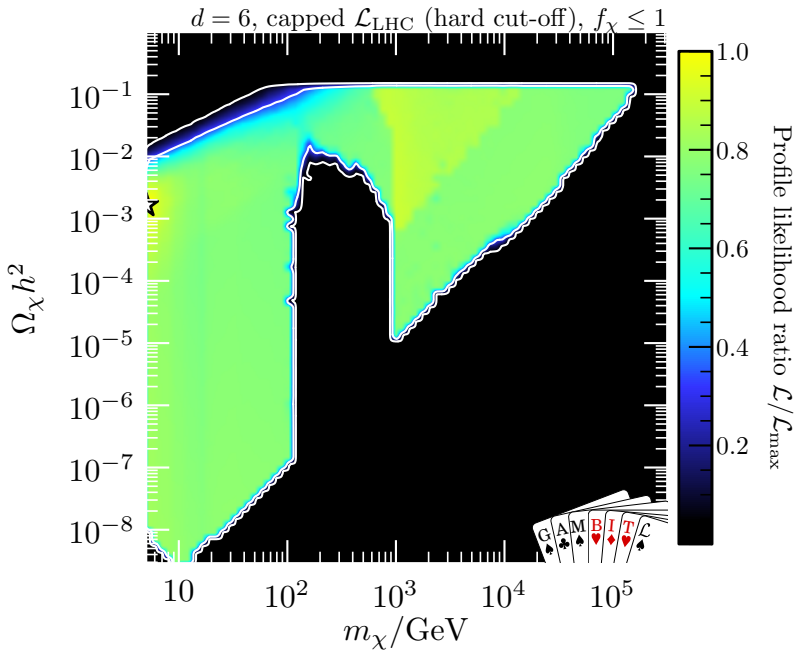

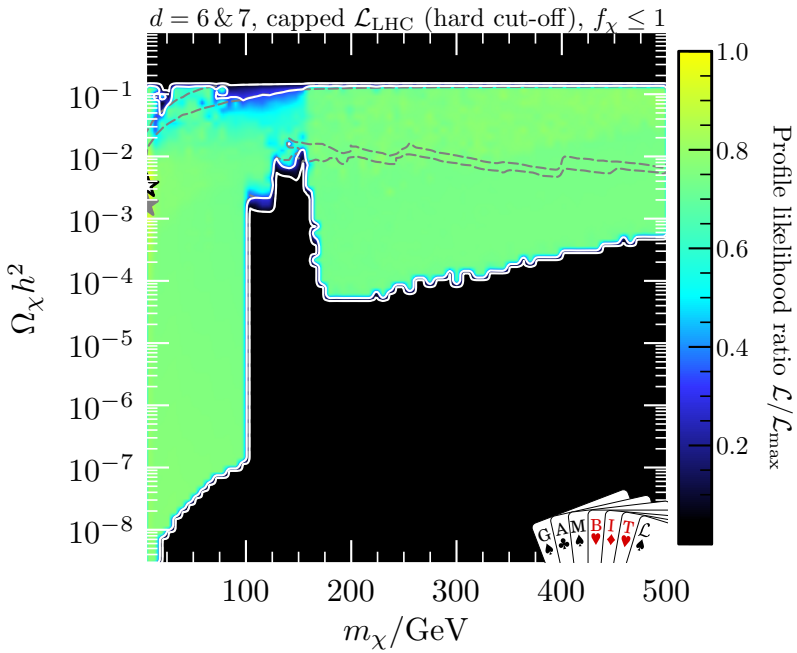

- For $d = 6$ and $m_\chi \lesssim 100\,\text{GeV}$, impossible to obtain $\Omega_\chi h^2 = 0.12$ with combined indirect and direct detection constraints.
- In $d = 6$ & 7, now possible to saturate relic density bound for small m_χ (and small Λ) thanks to suppressed signals from $\mathcal{Q}^{(7)}_{3,q}$ and $\mathcal{Q}^{(7)}_{7,q}$.

Supplementary results

Capped $\mathcal{L}_{\rm LHC}$ likelihood (hard cut-off), $f_\chi \leq 1$

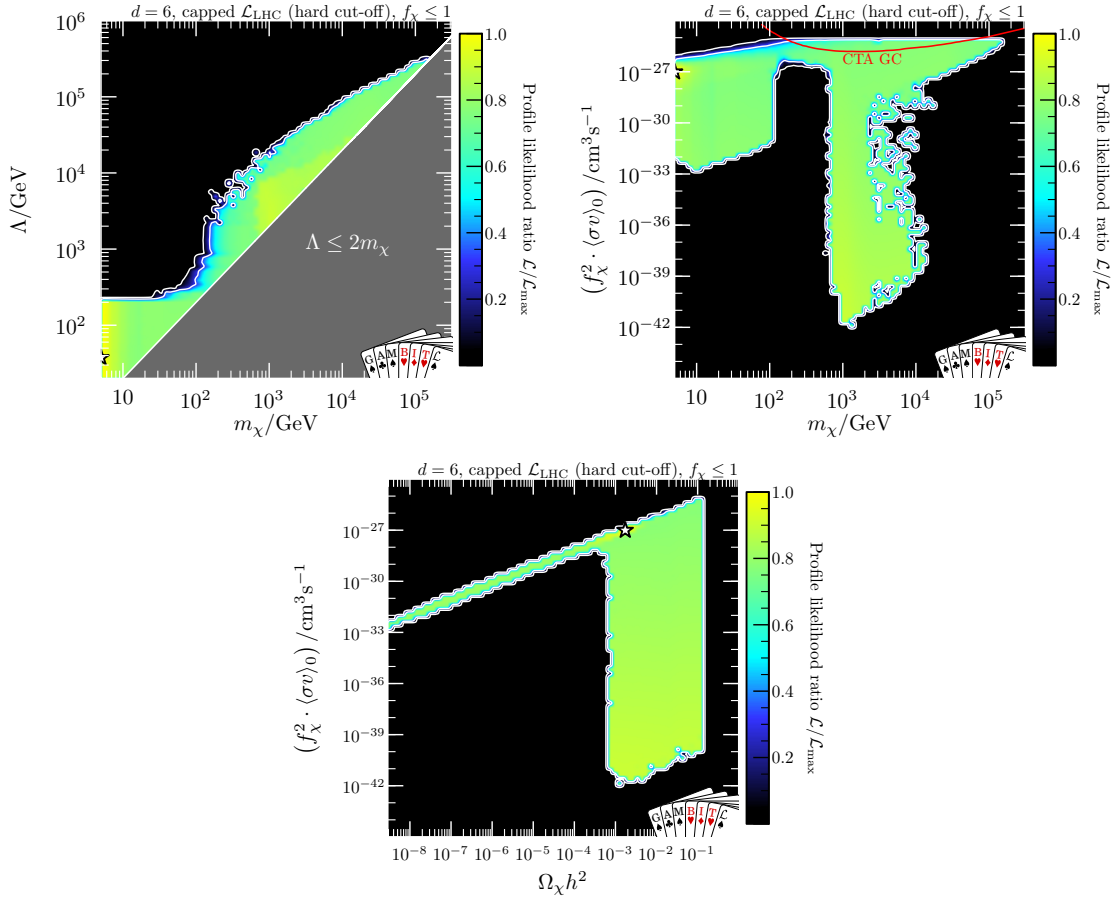

Left panel: $(m_\chi,\, \Lambda)$ plane. **Right panel**: $(m_\chi,\, f_\chi^2\langle\sigma v\rangle_0)$ plane.
Bottom panel: $(\Omega_\chi h^2,\, f_\chi^2\langle\sigma v\rangle_0)$ plane.

Capped $\mathcal{L}_{\rm LHC}$ likelihood (hard cut-off), $f_\chi \leq 1$

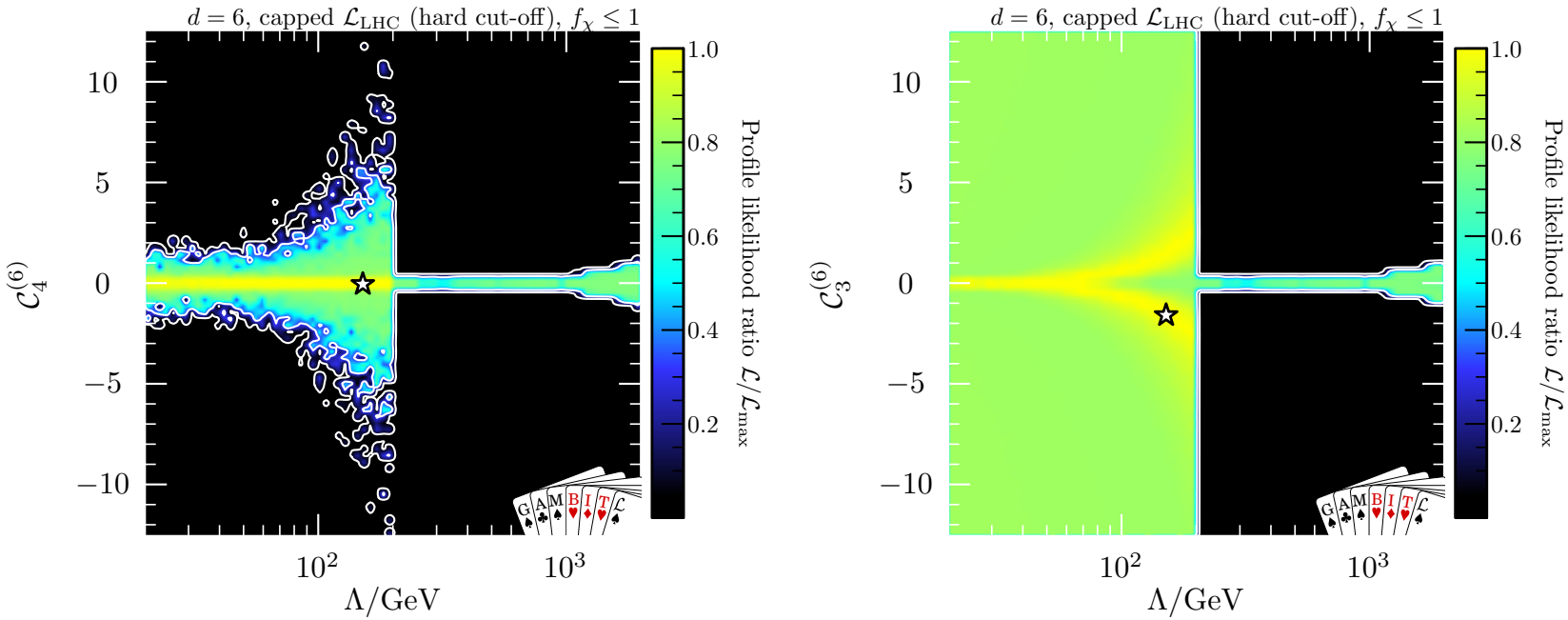

Left panel: $(m_\chi, \mathcal{C}_4^{(6)})$ plane. **Right panel**: $(m_\chi, \mathcal{C}_3^{(6)})$ plane.

Supplementary results

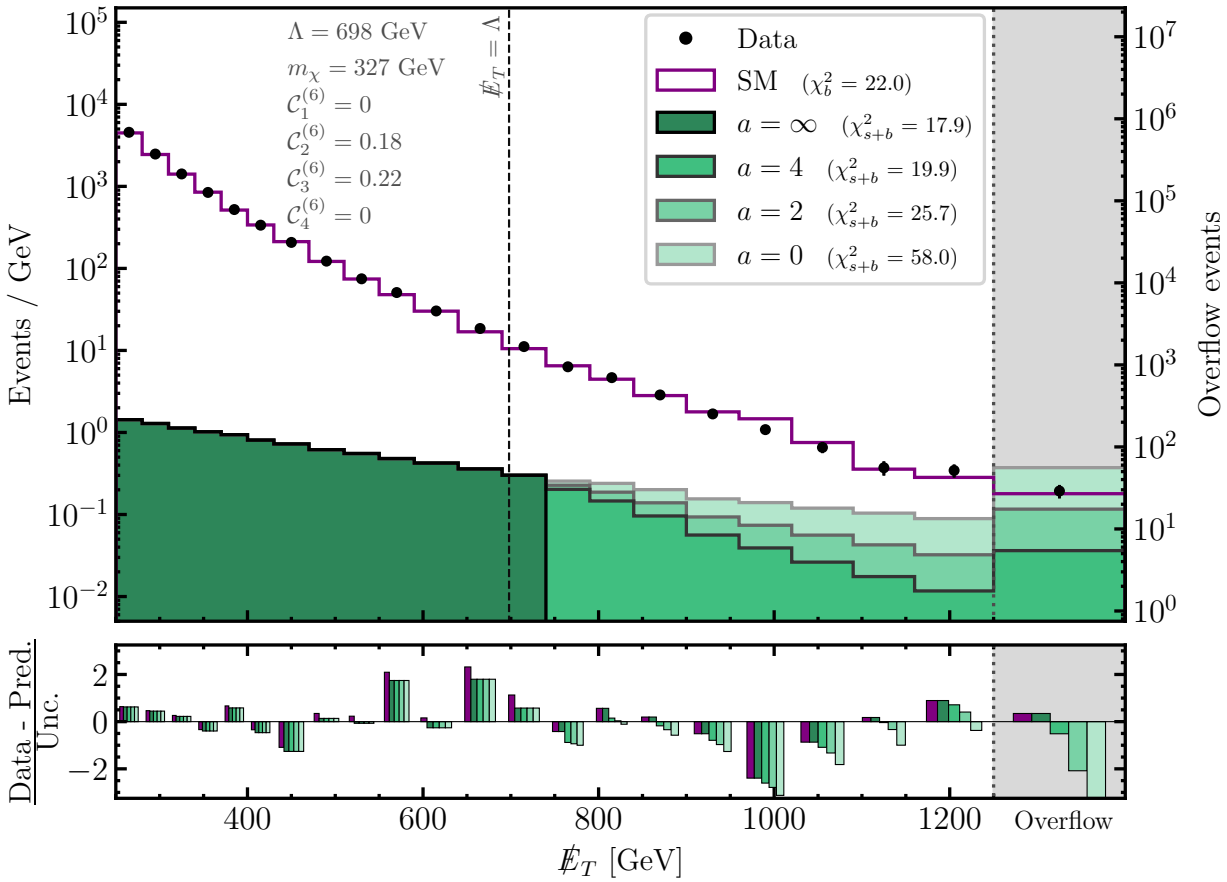

Top panel: Examples of missing transverse energy ($\not{E}_T$) spectrum for the CMS monojet search. **Bottom panel**: Pull ($\equiv$ (data - predicted)/uncertainty) per bin.

GAMBIT modules

1. **DarkBit** — *EPJC*, [arXiv:1705.07920]
   Relic density, indirect and direct detection.
2. **SpecBit**, **DecayBit** and **PrecisionBit** — *EPJC*, [arXiv:1705.07936]
   Spectrum calculation, decay widths and precision observables.
3. **FlavBit** — *EPJC*, [arXiv:1705.07933]
   Flavour physics, observables and likelihoods.
4. **ColliderBit** — *EPJC*, [arXiv:1705.07919]
   Collider observables and likelihoods.
5. **ScannerBit** — *EPJC*, [arXiv:1705.07959]
   Module for scanners and printers
6. **NeutrinoBit** — *EPJC*, [arXiv:1908.02302]
   Neutrino observables and likelihoods.
7. **CosmoBit** — *JCAP*, [arXiv:2009.03286]
   Cosmological observables and likelihoods.

Mixing and threshold corrections

- Threshold corrections when energy scale $\mu < m_q \rightarrow$ reduced degrees of freedom:

$$\mathcal{C}_{i,q}^{(7)} = \mathcal{C}_{i,q}^{(7)} - \mathcal{C}_{i+4,q}^{(7)} \, (i = 1,\, 2), \quad \mathcal{C}_{j,q}^{(7)} = \mathcal{C}_{j,q}^{(7)} + \mathcal{C}_{j+4,q}^{(7)} \, (j = 3,\, 4). \tag{6}$$

- Tensor operators $\mathcal{Q}_{9,q}^{(7)}$ and $\mathcal{Q}_{10,q}^{(7)}$ mix above EW scale $\Longrightarrow$ dim-5 dipole operators:

$$\mathcal{Q}_1^{(5)} = \frac{e}{8\pi^2}(\overline{\chi}\sigma_{\mu\nu}\chi)F^{\mu\nu}\,, \quad \mathcal{Q}_2^{(5)} = \frac{e}{8\pi^2}(\overline{\chi}i\sigma_{\mu\nu}\gamma_5\chi)F^{\mu\nu}\,. \tag{7}$$

- For $\Lambda > m_t$, $\mathcal{Q}_{9,10,t}^{(7)}$ gives a contribution to $\mathcal{Q}_{1,2}^{(5)}$ at one-loop level:

$$\mathcal{C}_{1,2}^{(5)}(m_Z) = \frac{4m_t^2}{\Lambda^2}\log\left(\frac{m_Z^2}{\Lambda^2}\right)\mathcal{C}_{9,10;t}^{(7)}(\Lambda)\,. \tag{8}$$

- Axial-vector top-quark current $\mathcal{Q}_{3,t}^{(6)}$ mixes into operators $\mathcal{Q}_{1,q}^{(6)}$:

$$\mathcal{C}_{1,u/d}^{(6)}(m_Z) = \mathcal{C}_{1,u/d}^{(6)}(\Lambda) + \frac{2s_w^2 \mp (3 - 6s_w^2)}{8\pi^2}\frac{m_t^2}{v^2}\log\left(\frac{m_Z^2}{\Lambda^2}\right)\mathcal{C}_{3,t}^{(6)}(\Lambda)\,.$$

ATLAS & CMS monojet searches

- Collider process: $pp \to \chi\chi j$ with missing transverse energy $\not{E}_T$.
- CMS and ATLAS monojet searches based on 36 fb^{-1} and 139 fb^{-1} of Run II data, respectively. G. Aad et al., [arXiv:2102.10874]; A. M. Sirunyan et al., *PRD*, [arXiv:1712.02345]
- Expected number of events in a given bin of $\not{E}_T$ distribution:

$$N = L \times \sigma \times (\epsilon A)\,. \tag{9}$$

- Produce separate interpolations of σ and (ϵA) based on output of MadGraph_aMC@NLO, interfaced to Pythia.
- Matching between MadGraph and Pythia performed according to CKKW prescription, and detector response simulation using Delphes.
- Only $\mathcal{C}_i^{(6)}$ and $\mathcal{C}_{i=1,\ldots,4}^{(7)}$ relevant for collider searches. Others suppressed by either PDFs (for heavy quarks) or mass term (for light quarks).
- Separate grids generated for operators that *do not* interfere. For $d = 6$, interference occurs between $\mathcal{Q}_{1,q}^{(6)}/\mathcal{Q}_{4,q}^{(6)}$ and $\mathcal{Q}_{2,q}^{(6)}/\mathcal{Q}_{3,q}^{(6)} \to$ parametrise tabulated grids by mixing angle θ as $\mathcal{C}_{1,2}^{(6)} = \sin\theta$ and $\mathcal{C}_{3,4}^{(6)} = \cos\theta$.

ATLAS & CMS monojet searches

- 22 and 13 exclusive signal regions in CMS and ATLAS monojet analyses, respectively.
- For CMS analysis, combine all signals using publicly available information. For ATLAS, only a single signal region used at once $\rightarrow$ maximise sensitivity by combining 3 highest $\not{E}_T$ bins.
- For CMS analysis, we have

$$\mathcal{L}_{\text{CMS}}(\boldsymbol{s},\boldsymbol{\gamma}) = \prod_{i=1}^{22}\left[\frac{(s_i+b_i+\gamma_i)^{n_i}\, e^{-(s_i+b_i+\gamma_i)}}{n_i!}\right] \frac{1}{\sqrt{\det 2\pi\Sigma}} e^{-\frac{1}{2}\boldsymbol{\gamma}^T\boldsymbol{\Sigma}^{-1}\boldsymbol{\gamma}}\,.$$

- Define profiled CMS likelihood ($\mathcal{L}_{\text{CMS}}(\boldsymbol{s}) \equiv \mathcal{L}_{\text{CMS}}(\boldsymbol{s},\hat{\hat{\boldsymbol{\gamma}}})$) by profiling over 22 nuisance parameters in $\boldsymbol{\gamma}$.
- For ATLAS analysis, $\mathcal{L}_{\text{ATLAS}}(s_i) \equiv \mathcal{L}_{\text{ATLAS}}(s_i,\hat{\hat{\gamma}}_i)$, where i = signal region with best expected sensitivity (one with lowest likelihood when $n_i = b_i$).
- Total LHC likelihood: $\ln\mathcal{L}_{\text{LHC}} = \ln\mathcal{L}_{\text{CMS}} + \ln\mathcal{L}_{\text{ATLAS}}$.

$$\Delta\ln\mathcal{L}_{\text{LHC}} = \ln\mathcal{L}_{\text{LHC}}(\boldsymbol{s}) - \ln\mathcal{L}_{\text{LHC}}(\boldsymbol{s}=\boldsymbol{0})\,, \tag{10}$$

$$\Delta\ln\mathcal{L}^{\text{cap}}_{\text{LHC}}(\boldsymbol{s}) = \min\left[\Delta\ln\mathcal{L}_{\text{LHC}}(\boldsymbol{s}), \Delta\ln\mathcal{L}_{\text{LHC}}(\boldsymbol{s}=\boldsymbol{0})\right]\,. \tag{11}$$

Nuisance parameters

Nuisance parameter		**Value** ($\pm 3\sigma$ **range**)
Local DM density	ρ_0	0.2–$0.8\,\mathrm{GeV\,cm^{-3}}$
Most probable speed	v_{peak}	$240\,(24)\,\mathrm{km\ s^{-1}}$
Galactic escape speed	v_{esc}	$528\,(75)\,\mathrm{km\ s^{-1}}$
Running top mass ($\overline{\mathrm{MS}}$ scheme)	$m_t(m_t)$	$162.9\,(6.0)\,\mathrm{GeV}$
Pion-nucleon sigma term	$\sigma_{\pi N}$	$50\,(45)\ \mathrm{MeV}$
Strange quark contrib. to nucleon spin	Δs	$-0.035\,(0.027)$
Strange quark nuclear tensor charge	g_T^s	$-0.027\,(0.048)$
Strange quark charge radius of the proton	r_s^2	$-0.115\,(0.105)\ \mathrm{GeV^{-2}}$

Table 1: List of nuisance parameters that are varied simultaneously with the DM EFT model parameters.

Type of interactions

	SI scattering	SD scattering	Annihilations
Dimension-6 operators			
$\mathcal{Q}^{(6)}_{1,q} = (\overline{\chi}\gamma_\mu\chi)(\overline{q}\gamma^\mu q)$	unsuppressed	—	s-wave
$\mathcal{Q}^{(6)}_{2,q} = (\overline{\chi}\gamma_\mu\gamma_5\chi)(\overline{q}\gamma^\mu q)$	suppressed	—	p-wave
$\mathcal{Q}^{(6)}_{3,q} = (\overline{\chi}\gamma_\mu\chi)(\overline{q}\gamma^\mu\gamma_5 q)$	—	suppressed	s-wave
$\mathcal{Q}^{(6)}_{4,q} = (\overline{\chi}\gamma_\mu\gamma_5\chi)(\overline{q}\gamma^\mu\gamma_5 q)$	—	unsuppressed	s-wave $\propto m_q^2/m_\chi^2$
Dimension-7 operators			
$\mathcal{Q}^{(7)}_{1} = \frac{\alpha_s}{12\pi}(\overline{\chi}\chi)G^{a\mu\nu}G^a_{\mu\nu}$	unsuppressed	—	p-wave
$\mathcal{Q}^{(7)}_{2} = \frac{\alpha_s}{12\pi}(\overline{\chi}i\gamma_5\chi)G^{a\mu\nu}G^a_{\mu\nu}$	suppressed	—	s-wave
$\mathcal{Q}^{(7)}_{3} = \frac{\alpha_s}{8\pi}(\overline{\chi}\chi)G^{a\mu\nu}\widetilde{G}^a_{\mu\nu}$	—	suppressed	p-wave
$\mathcal{Q}^{(7)}_{4} = \frac{\alpha_s}{8\pi}(\overline{\chi}i\gamma_5\chi)G^{a\mu\nu}\widetilde{G}^a_{\mu\nu}$	—	suppressed	s-wave
$\mathcal{Q}^{(7)}_{5,q} = m_q(\overline{\chi}\chi)(\overline{q}q)$	unsuppressed	—	p-wave $\propto m_q^2/m_\chi^2$
$\mathcal{Q}^{(7)}_{6,q} = m_q(\overline{\chi}i\gamma_5\chi)(\overline{q}q)$	suppressed	—	s-wave $\propto m_q^2/m_\chi^2$
$\mathcal{Q}^{(7)}_{7,q} = m_q(\overline{\chi}\chi)(\overline{q}i\gamma_5 q)$	—	suppressed	p-wave $\propto m_q^2/m_\chi^2$
$\mathcal{Q}^{(7)}_{8,q} = m_q(\overline{\chi}i\gamma_5\chi)(\overline{q}i\gamma_5 q)$	—	suppressed	s-wave $\propto m_q^2/m_\chi^2$
$\mathcal{Q}^{(7)}_{9,q} = m_q(\overline{\chi}\sigma^{\mu\nu}\chi)(\overline{q}\sigma_{\mu\nu}q)$	loop-induced	unsuppressed	s-wave $\propto m_q^2/m_\chi^2$
$\mathcal{Q}^{(7)}_{10,q} = m_q(\overline{\chi}i\sigma^{\mu\nu}\gamma_5\chi)(\overline{q}\sigma_{\mu\nu}q)$	loop-induced	suppressed	s-wave $\propto m_q^2/m_\chi^2$

Table 2: Full list of dimension-6 and 7 operators included in our study, and the types of interactions they induce. Here SI (SD) = spin-independent (spin-dependent) DM-nucleon interaction.

Best-fit points

LHC likelihood	Relic density constraint	$2\Delta \ln \mathcal{L}$	Best-fit m_χ (GeV)	Best-fit Λ (GeV)	Best-fit constrained coupling combination(s) (TeV^{-2})
Capped	Upper bound	0.3	5.0	< 200	$\lvert\mathcal{C}_3^{(6)}\rvert/\Lambda^2 = 67$
Capped	Saturated	-0.5	500	> 1000	$\lvert\mathcal{C}_2^{(6)}\rvert/\Lambda^2 = 0.22$ $\lvert\mathcal{C}_3^{(6)}\rvert/\Lambda^2 = 0.041$
Full (hard cut-off)	Upper bound	2.2	500	> 1250	$\lvert\mathcal{C}_3^{(6)}\rvert/\Lambda^2 = 0.14$
Full (smooth cut-off)	Upper bound	2.6	320	640	$\lvert\mathcal{C}_3^{(6)}\rvert/\Lambda^2 = 0.18$
Full (hard cut-off)	Saturated	1.9	500	> 1250	$\lvert\mathcal{C}_3^{(6)}\rvert/\Lambda^2 = 0.047$ $\sqrt{(\mathcal{C}_2^{(6)})^2 + (\mathcal{C}_4^{(6)})^2}/\Lambda^2 = 0.15$
Full (smooth cut-off)	Saturated	2.0	420	840	$\lvert\mathcal{C}_3^{(6)}\rvert/\Lambda^2 = 0.052$ $\sqrt{(\mathcal{C}_2^{(6)})^2 + (\mathcal{C}_4^{(6)})^2}/\Lambda^2 = 0.23$

Table 3: Best-fit points from our various scans involving dimension-6 operators with restricted parameter ranges ($5\,\text{GeV} \leq m_\chi \leq 500\,\text{GeV}$ and $20\,\text{GeV} \leq \Lambda \leq 2\,\text{TeV}$). Here we only quote the combination that is well-constrained rather than each parameter individually.